Adhesion Properties of Glow-Discharge-Plasma-Treated Polyethylene Surface

A. YU. KUZNETSOV, V. A. BAGRYANSKY, and A. K. PETROV*

Institute of Chemical Kinetics and Combustion, 630090, Novosibirsk, Russia

SYNOPSIS

A geometric method proposed by Kaelble and Moacanin for analyzing energetic characteristics of solid surfaces is discussed. It is shown that a number of characteristics can be presented in a visual geometric form. The method is applied to the analysis of adhesion in a three-component system. Results of the analysis, concerned with the problem of creation of biocompatible materials, support the Andrade hypothesis that materials with zero interfacial tension of their water–solid interface show maximum biocompatibility. Data are obtained on wetting of polyethylene by different liquids before and after glow discharge plasma treatment. The analysis of these data in terms of geometric method shows the plasma treatment increased the polar component of the polymer surface energy to change the surface adhesiveness toward probable enhancement of polymer biocompatibility. That is consistent with available data on glow-discharge-treatment enhancement of biocompatibility for a number of polymers. © 1993 John Wiley & Sons, Inc.

INTRODUCTION

The ability of the polymer surface to adhere to other substances is important in a number of applications, e.g., in painting, coating, and production of polymeric membranes. Polymers are widely used in medicine where their biocompatibility is of great importance. By biocompatibility, we mean the properties of an implant material, which afford its long service. The biocompatibility of an implanted polymeric material depends on a number of its properties. Of most importance for biocompatibility are the energetic characteristics of a polymer, which determine its wettability and adhesion. The question of the energetic characteristics of a polymer, optimum for its biocompatibility, has been the focus of much attention.[1-12] However, this problem has not been hitherto solved. It has been assumed[2-4] that materials that do not adsorb proteins, enzymes, cells, and other elements of biologic liquids show high biocompatibility. For example, Ikada et al.[3] suppose that a polymer that does not adsorb blood proteins should be resistant to thromb formation. Another example concerns intraocular and contact lenses. The high adhesion of eye liquid components leads to lens dimness.[5] The opposite hypothesis has also been proposed. Thus, Paul and Sharma[6] assume that a polymer is biocompatible if it exhibits a high ability to adsorb albumin and a low ability to adsorb other proteins. Kaelble and Moacanin[1] state that the high biocompatibility is ensured when the implant surface is coated with a layer of adsorbed protein. Indeed, there are implants for which the adsorption of protein, resulting in coating by connective tissue, is desirable, e.g., fabric blood vessels wherein such coating leads to formation of pseudointima. Anyway, for estimation of the biocompatibility of a polymer, it seems to be reasonable to analyze its adhesion properties.

In this work, we discuss the possibilities of the geometric method[1] on the analysis of energetic characteristics of surfaces participating in the adhesive joint. It is shown that adhesion characteristics can be presented simply and visually.

This work is concerned with the problem of the energetic characteristics of implant materials, optimum for their biocompatibility. The problem is discussed in terms of the above hypothesis about

* To whom correspondence should be addressed.

Journal of Applied Polymer Science, Vol. 47, 1175–1184 (1993)
 CCC 0021-8995/93/071175-10

the maximum biocompatibility of nonadsorbing materials. The geometric method is used.

One of the methods of surface modification that enhance the polymer biocompatibility is the glow discharge plasma treatment.[7,13-15] We have compared experimental energetic characteristics of the polyethylene (PE) surface prior to and after treatment in the air glow discharge plasma. The analysis performed using the geometric method shows that such a treatment should decrease the adhesion of biological liquid components to PE surface, which can lead to the enhancement of polymer biocompatibility.

ENERGETIC CHARACTERISTICS OF SURFACES: WETTING AND ADHESION

The strength of adhesive joints of substances is determined by energetic characteristics of partners. We will discuss the present knowledge of the relationship between these characteristics and adhesion strength parameters.

The most widespread way for determining the energetic characteristics of a solid surface is measuring the equilibrium contact angle between the solid and wetting liquid. The value of this angle is set by the Young equation:

$$\gamma_{lv} \cos \theta = \gamma_{sv} - \gamma_{ls} - \pi_l \qquad (1)$$

where γ_{lv} and γ_{sv} are the free energies of the liquid and solid surfaces in the saturated vapor of the liquid, γ_{ls} is the liquid–solid interfacial tension, and π_l is the spreading pressure of liquid molecules adsorbed on the solid. Ignoring the interaction of the condensed phase surfaces with vapor and the value π_l that is negligible for most polymers,[16] eq. (1) can be rewritten as follows:

$$\gamma_l \cos \theta = \gamma_s - \gamma_{ls} \qquad (2)$$

In eq. (2), only γ_l and $\cos \theta$ are susceptible to direct measurement. To determine γ_s and γ_{ls}, which characterize solid surfaces, one needs additional information about their interrelation. This information may be obtained using knowledge on the nature of intermolecular interactions.

Owens and Wendt[17] proposed an extended version of the Fowkes equation:

$$\gamma_{ls} = \gamma_l + \gamma_s - 2((\gamma_l^d \gamma_s^d)^{0.5} + (\gamma_l^p \gamma_s^p)^{0.5}) \qquad (3)$$

where γ_l^d and γ_s^d are the contributions of dispersion forces and γ_l^p and γ_s^p are the contributions of polar forces to free surface energies. Using eq. (2), we can rewrite eq. (3) as follows:

$$\gamma_l(1 + \cos \theta) = 2((\gamma_l^d \gamma_s^d)^{0.5} + (\gamma_l^p \gamma_s^p)^{0.5}) \qquad (4)$$

Then, using the equation for adhesion energy,

$$W_{ls} = \gamma_l + \gamma_s - \gamma_{ls} \qquad (5)$$

eq. (3) can be rewritten in the following form:

$$W_{ls} = 2((\gamma_l^d \gamma_s^d)^{0.5} + (\gamma_l^p \gamma_s^p)^{0.5}) \qquad (6)$$

Equation (3) was validated[17] by the fact that the dispersion interaction and dipole orientation interaction of different molecules are expressed via geometric means of corresponding individual parameters of the molecules. However, the wide use of the extended Fowkes equation cannot free it from criticism. In particular, the ignorance of induction interaction in derivation of this equation gives an error, which has not been estimated. Besides, the assumption about geometric means holds for one-component substances in a point-dipole approximation. The applicability of this approximation to complex substances, e.g., to polymers, needs special consideration.

Let us show that extended Fowkes eqs. (3), (4), and (6) also hold in the case when the induction interaction is taken into account. These equations will hold for complex molecules and multicomponent systems if the latter can be described as sets of different kinds of point dipoles with limited mobility, so local dipole concentrations are independent of the distance from the surface. Such dipoles can be various simple molecules or groups of complex molecules with specified values of permanent dipole moment and polarizability. It is difficult to estimate the validity of this assumption, proceeding from physical considerations. One may, however, note an analogy with a well-known method for estimating chemical shifts, which is successfully used in NMR spectroscopy.[18]

Consider the description of surface energetic characteristics in terms of the above assumptions. Girifalco and Good[19] calculated the adhesion energy W_{ab} of two semi-infinite one-component phases a and b having a plane contact. It was assumed that the interaction of phase molecules was described by the Lennard–Jones potential and the distance between contacting planes was equilibrium. It has been found that

$$W_{ab} = (\pi/16)(n_a n_b/d_{ab}^2)A_{ab} \qquad (7)^\dagger$$

† The multiplier $\pi/16$ is erroneously lacking in this equation in Ref. 19.

where n_a and n_b are the densities of phases a and b, respectively, in molecules per unit volume; d_{ab} is the equilibrium distance between the planes; and A_{ab} is the attraction constant of the Lennard–Jones potential of the molecules of a and b phases. Note that the attraction in this potential corresponds to the interaction of molecules as point dipoles, both permanent and induced. To generalize eq. (7) to the case of phases consisting of different kinds of dipoles, it suffices to consider dipoles of each kind as phase components nested in each other. On the assumption of the homogeneous spatial distributions of particles of each kind, the interaction between phase components obeys eq. (7). Then, the adhesion energy will be the sum of contributions of phase components:

$$W_{ab} = (\pi/16)(n_a n_b/d_{ab}^2) \sum_{i,j} g_i^a g_j^b A_{ij} \qquad (8)$$

where g_i^a and g_j^b are the shares of dipoles, respectively, of i and j kinds for a and b phases, and A_{ij} is the attraction constant for i and j dipoles. According to London's and Debye–Keesom's theories, A_{ij} can be expressed as follows[20]:

$$A_{ij} = \frac{3}{2}\frac{I_i I_j}{I_i + I_j}\alpha_i\alpha_j + \frac{2}{3kT}p_i^2 p_j^2 + \alpha_i p_j^2 + \alpha_j p_i^2 \qquad (9)$$

where I is the mean electron energy close to the ionization potential; α, the polarizability; and p, the permanent dipole moment of corresponding particle. The first summand in eq. (9) corresponds to the dispersion interaction; the second summand, to the dipole–dipole interaction; and the last two terms, to the induction interaction. For a pair of similar particles,

$$A_{ii} = \frac{3}{4}I_i\alpha_i^2 + \frac{2}{3kT}p_i^4 + 2\alpha_i p_i^2 = A_i^d + A_i^p \qquad (10)$$

Here A_i^d means the contribution of dispersion forces to the constant A_{ii}, i.e., the first summand in eq. (10), and A_i^p denotes the contribution of polar forces, i.e., the two latter terms in eq. (10). The values A_i^d and A_i^p characterize the interaction ability of the i-kind particles. The constant A_{ij} can be expressed via A_i^d, A_i^p and A_j^d, A_j^p in the form

$$A_{ij} = \left(\frac{2(I_iI_j)^{0.5}}{I_i + I_j} + \frac{2kT}{(I_iI_j)^{0.5}}\right)(A_i^d A_j^d)^{0.5} + \left(A_i^p + \frac{2kT}{I_i}A_i^d\right)^{0.5}\left(A_j^p + \frac{2kT}{I_j}A_j^d\right)^{0.5} \qquad (11)$$

The value $(2kT)/I$ at room temperature is below $5\cdot10^{-2}$ and, hence, can be neglected. Besides, $[2(I_iI_j)^{0.5}]/(I_i + I_j) \approx 1$ since the geometric mean differs from the arithmetic mean only at large difference in averaged values. The ionization potentials of organic molecules are, however, close. Then,

$$A_{ij} = (A_i^d A_j^d)^{0.5} + (A_i^p A_j^p)^{0.5} \qquad (12)$$

Substitution of eq. (12) into eq. (8) and change of the sum of products in eq. (8) for the product of sums gives the following expression for adhesion energy:

$$W_{ab} = (\pi/16)(n_a n_b/d_{ab}^2)(\langle(A^d)^{0.5}\rangle_a\langle(A^d)^{0.5}\rangle_b + \langle(A^p)^{0.5}\rangle_a\langle(A^p)^{0.5}\rangle_b) \qquad (13)$$

where angular brackets $\langle\ \rangle_{a,b}$ designate the averaging of bracketed expression over the distribution of dipole properties in the phases a and b. If the phases are identical, expression (13) is transformed to the expression for cohesion energy:

$$W_{aa} = (\pi/16)(n_a^2/d_{aa}^2) \times (\langle(A^d)^{0.5}\rangle_a^2 + \langle(A^p)^{0.5}\rangle_a^2) \qquad (14)$$

Since

$$W_{aa} = 2\gamma_a \qquad (15)$$

the contributions of dispersion and polar forces to the surface energy $\gamma_a = \gamma_a^d + \gamma_a^p$ can be isolated as follows:

$$\gamma_a^d = (\pi/32)(n_a^2/d_{aa}^2)\langle(A^d)^{0.5}\rangle_a^2 \qquad (16)$$

$$\gamma_a^p = (\pi/32)(n_a^2/d_{aa}^2)\langle(A^p)^{0.5}\rangle_a^2 \qquad (17)$$

Then, eq. (13) can be rewritten in the form

$$W_{ab} = 2((\gamma_l^d\gamma_s^d)^{0.5} + (\gamma_l^p\gamma_s^p)^{0.5})(d_{aa}d_{bb}/d_{ab}^2) \qquad (18)$$

Equation (18) coincides with a form of the extended Fowkes eq. (6) at $d_{aa}d_{bb}/d_{ab}^2 \approx 1$. According to qualitative considerations, this condition is approximately true. Thus, it can be concluded that the extended Fowkes equation holds true in the case when the induction interaction is taken into account and can be employed in the description of more complex systems.

This equation allows one to calculate all needed energetic characteristics for given dispersion and polar components of the surface energy of interacting substances. The components are determined by

eq. (4) from a series of experimental data on wetting of substrates by different liquids. γ_l^d and γ_l^p for a number of liquids have been determined in this manner.[17,21-23] With these numerical values available, to determine γ_s^d and γ_s^p for a solid, it suffices to measure the contact angles of the solid surface with two (or more) liquids and then calculate the needed values using eq. (4).

This method is not the only one used for determining the energetic characteristics of solid surfaces. The approach suggested by Good and Girifalco[19,24] is based on the same concept of intermolecular interactions. The parameters determining these interactions are used in calculation of the quantity Φ that is set by the expression

$$\Phi = W_{ls}/(W_{ll}W_{ss})^{0.5} \tag{19}$$

Then, the solid surface energy can be derived from the equation

$$\gamma_s = \gamma_l(1 + \cos\theta)^2/4\Phi^2 \tag{20}$$

which is a combination of eqs. (2), (5), (15), and (19). The advantage of this method is that it requires no assumption of the equality of ionization potentials of interacting substances. The gravest disadvantage of the method is that to calculate Φ one should know all values that characterize the molecular interaction [eqs. (7), (9), and (19)] of both substances. In fact, such information is not always available. This problem is solved either by setting[24] $\Phi = 1$ or by estimating this parameter from empirical relationship.[25]

A slightly different approach is suggested by Wu.[26] In terms of this approach, the adhesion energy is supposed to be a sum of harmonic means of the dispersion and polar components of surface energy:

$$W_{ls} = 4\gamma_l^d\gamma_s^d/(\gamma_l^d + \gamma_s^d) + 4\gamma_l^p\gamma_s^p/(\gamma_l^p + \gamma_s^p) \tag{21}$$

In this expression, the first term can be obtained on the assumption of equal polarizabilities of interacting substances. The form of the second term is taken arbitrarily (by analogy with the first one).

Comparison of eqs. (6) and (21) shows that the difference of the approach of Owens and Wendt from that of Wu is in the type of averaging: The former uses the geometric means of surface energy components, whereas the latter employs the harmonic means. These two types of averaging can give essentially different values only if the values to be averaged are very different. For example, if two values differ from each other by no more than a factor of 4, the difference between their geometric and harmonic means is no more than 20%. This perhaps accounts for the fact that the difference in γ^d and γ^p values obtained using these two approaches is within the experimental error.[26,27]

A comparison of the described approaches has allowed us to conclude that the geometric mean formalism specified by eqs. (3), (4), and (6) is a method most suitable for experimental data processing and, at the same time, the least vulnerable from the viewpoint of the adopted assumptions.

GEOMETRIC APPROACH TO ANALYZING THE ENERGETIC CHARACTERISTICS OF A SURFACE

Kaelble and Moacanin[1] proposed a geometric method for the analysis of adhesion. In terms of this method, the surface energy values γ_l and γ_s are related to two points on a $(\gamma^p)^{0.5}$ vs. $(\gamma^d)^{0.5}$ plane (see Fig. 1). Designate these points by the letters L and S; then, the vectors going from the origin of coordinates to the points will be **OL** and **OS**, respectively. In this case, eqs. (3), (4), and (6), as well as some other expressions derived from these equations, allow visual geometric interpretation. Itemize the properties and possibilities of such a representation:

(1) Surface energy. γ_l and γ_s are equal to the squares of **OL** and **OS** lengths, respectively:

$$\gamma_l = OL^2, \quad \gamma_s = OS^2 \tag{22}$$

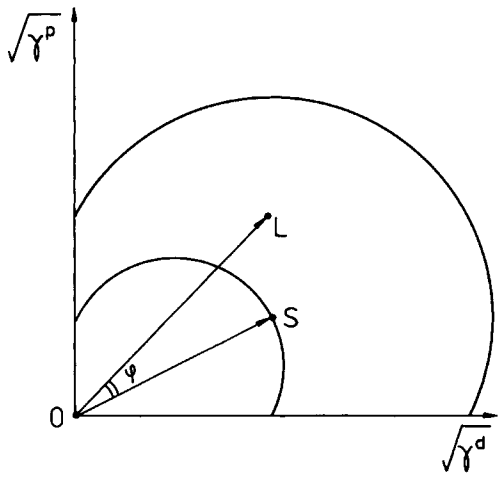

Figure 1 Energetic characteristics of a solid (point S) and a wetting liquid (point L) in $(\gamma^p)^{0.5}$ vs. $(\gamma^d)^{0.5}$ coordinates. Area within the small circle, liquids totally wetting the solid; area out of the large circle, nonwetting liquids.

(2) Adhesion energy. It follows from eq. (6) that

$$W_{ls} = 2 \cdot \mathbf{OL} \cdot \mathbf{OS} \tag{23}$$

where $\mathbf{OL} \cdot \mathbf{OS}$ is the scalar product of **OL** and **OS**, which is maximum for the vectors of given lengths when their directions coincide. For liquids with the same γ_l (and, hence, OL), the maximum adhesion energy will be observed in the liquid that shows the same ratio between the dispersion and polar forces as the solid does.

(3) Interfacial tension γ_{ls}. It follows from eqs. (3) and (22) and the available expression for the sides of the triangle LOS:

$$LS^2 = OL^2 + OS^2 - 2 \cdot \mathbf{OL} \cdot \mathbf{OS} \tag{24}$$

that

$$\gamma_{ls} = LS^2 \tag{25}$$

(4) Total wetting. Using eqs. (22), (24), and (25), the condition of total wetting $\gamma_l \leq \gamma_s - \gamma_{ls}$ can be presented as

$$OL \leq \mathbf{OL} \cdot \mathbf{OS}/OL \tag{26}$$

The right side of eq. (26) is the projection of **OS** onto **OL**. Hence, this condition can be satisfied only by liquids whose L points are on and within the circle with a center in the middle of **OS** and the radius $OS/2$ (Fig. 1). Equality in eq. (26) defines the properties of a liquid with a critical, for a given solid, surface tension γ_c.[28] At total wetting, $\gamma_c \leq \gamma_s$, the equality being observed only if the ratio between the dispersion and polar forces of intermolecular interaction is the same for the liquid and solid.

(5) Nonwetting liquids. Assuming in eq. (4) $\cos\theta < 0$ and using eqs. (5), (22), and (23), obtain the condition

$$OL > 2 \cdot \mathbf{OS} \cdot \mathbf{OL}/\mathrm{OL} \tag{27}$$

This condition is met by points being out of the circle of the radius OS, centered at S (Fig. 1).

(6) The parameter Φ. Using Φ definition (19) and eqs. (15), (22), and (23), write

$$\Phi = \mathbf{OL} \cdot \mathbf{OS}/(OL \cdot OS) = \cos\varphi \tag{28}$$

where φ is the angle between **OL** and **OS** (Fig. 1). The widely used assumption $\Phi = 1$ is seen to be true only at $\varphi = 0$, i.e., at equal ratio between the dispersion and polar forces in the liquid and solid.

(7) Adhesion energy in a three-component system. Let a solid corresponding to a certain point S be dipped into a buffer liquid corresponding to a point B (Fig. 2). The system also includes drops of a liquid L insoluble in the buffer liquid. Express the adhesion energy $W_{ls(b)}$ of L drops on the S surface surrounded by the buffer liquid B:

$$W_{ls(b)} = \gamma_{lb} + \gamma_{bs} - \gamma_{ls} \tag{29}$$

Substituting in eq. (29) expressions similar to (25) for each interfacial tension and using an equation similar to the eq. (24) for the sides of the triangle LBS, obtain

$$W_{ls(b)} = 2 \cdot \mathbf{BL} \cdot \mathbf{BS} \tag{30}$$

Equation (30) is similar to eq. (23) and they coincide if the buffer is a hypothetical liquid O with zero surface energy. Kaelble and Moacanin[1] gave an interpretation of adhesion energy value, which is different from that suggested by eq. (30). It can be shown, however, that these two interpretations are completely equal. At the same time, in our opinion, scalar product (30) is a more visual and easy-to-analyze form of representation.

Expression (30) permits one to estimate which properties of the solid surface are preferable from

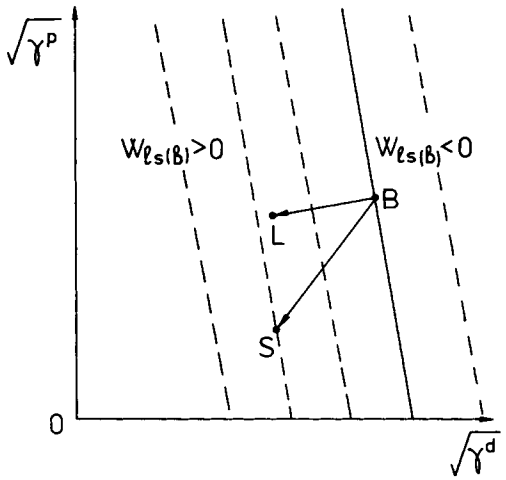

Figure 2 A $(\gamma^p)^{0.5}$ vs. $(\gamma^d)^{0.5}$ plot for the analysis of adhesion energy $W_{ls(b)}$ in a three-component system. Solid straight line separates the regions of positive and negative adhesion energy values of a liquid L at the surface of a solid S surrounded by a buffer liquid B. Broken lines, isolines of S points with a constant adhesion energy $W_{ls(b)}$.

the viewpoint of adhesion in such a system. It is evident that the isolines on which S points give the same value of $W_{ls(b)}$ are straight lines perpendicular to **BL** (Fig. 2). The line passing through point B corresponds to zero adhesion energy. The straight lines on the left of this line correspond to the positive adhesion energy, and on the right, to the negative adhesion energy.

Thus, the geometric approach allows simple presentation of the energetic characteristics and adhesion properties of surfaces. This approach is most helpful in studying three-component systems for which it is difficult to perform a similar analytical consideration because of the awkwardness of the formulae.[3] The analysis of adhesion in a three-component system has a direct bearing on the problem of the creation of biocompatible materials. Andrade et al.[2] proposed a hypothesis that materials with zero interfacial tension of the water–polymer surface have maximum biocompatibility. The authors[2] claim that protein adsorption at the polymer surface in this case is absent. The geometric approach confirms this assumption about the correlation between zero interfacial energy and the absence of adsorption.

Consider a three-component system with water as a buffer liquid. Since the energetic characteristics of biologic liquids are close to those of water, such a system models well the contact of a polymer with a living organism. The substance L will be considered as a model of biologic liquid components whose adhesion determines the biocompatibility of the solid S (Fig. 2). The interfacial tension γ_{bs} of the water–solid interface becomes zero at $BS = 0$ [eq. (25)]. In this case, as follows from eq. (30), the adhesion energy of any substance at the solid surface in aqueous medium is zero. In terms of the hypothesis mentioned in the Introduction, this situation corresponds to the maximum biocompatibility of material.

EXPERIMENTAL TECHNIQUE

Polyethylene (PE) tubes (length 40 mm, bore diameter 0.6 mm) cut from subclavian catheters obtained from "Synthesis" (Kurgan, Russia) were used. Note that for these catheters Gonchar et al.[14] observed increased resistance to thromb formation after glow discharge air plasma treatment. The surface tensions (from the literature) of the liquids used are given in Table I. We chose the liquids whose surface tensions were available and that did not wet completely the samples under investigation. Prior to measurement, all the liquids were purified by distillation.

The experimental setup for glow discharge treatment is presented schematically in Figure 3. The samples were treated in a cylindrical glass reactor, 45 mm in diameter and 1.1 L in volume, with two nickel electrodes. The distance between the electrodes was 600 mm. The reactor was equipped with a manometer and two dripcocks, one for evacuation and the other for controlling velocity of the air flow. The electrodes were connected to a stabilized power supply (direct current) to maintain the discharge glow in the reactor. A hurling vacuum pump was used. The system was equipped with a liquid nitrogen trap to prevent the permeation of oil vapor into the reactor. Prior to treatment, PE tubes were boiled in dichloromethane for 2 h and then dried in a vacuum desiccator cabinet. A tube to be treated was placed in the center of the reactor, along its axis. The reactor was evacuated down to a pressure of 10^{-3} Torr, which was sustained for 4 h. Then, the discharge was switched on. The discharge parameters were the following: pressure in the reactor, 0.6 Torr; velocity of air flow through the reactor, $1.9 \cdot 10^{-4}$ mol/min; discharge current, 8 mA; and exposure time, 20 min.

The contact angle of the interior surface of the tube was determined by the height h of the wetting liquid in the tube dipped upright into the liquid, using the well-known formula

$$\cos \theta = hr\rho g/(2\gamma_l)$$

where r is the tube radius; ρ, the liquid density; and g, the gravitational acceleration. h values turned out to be the same (within the experimental accuracy ± 0.5 mm) for the cases when the liquid rose in the tube and when it flew out of the preliminarily filled tube.

EXPERIMENTAL RESULTS

For the pair initial PE–water, $\cos \theta = (-0.28 \pm 0.03)$. Plasma treatment led to increased wettability of PE by water. After treatment, $\cos \theta = (0.6 \pm 0.03)$. This value coincides with that for a flat sample of the same material treated under the same conditions. The latter value of $\cos \theta$ is independent of the tube position in the reactor and of the distance from the wetted section to the tube ends. This has been proved experimentally: 40 mm-long tubes were placed on the reactor walls both along the reactor axis and perpendicularly to it, suspended by thin

Table I Liquids Used, Their Surface Tensions, and Surface Tension Dispersion Components (References and Our Data), Contact Angle Cosines for Initial and Discharge-treated PE

No.	Substance	γ_l (erg/cm^2)	γ_l^d (erg/cm^2), Refs. 17, 21–23	γ_l^d (erg/cm^2), Our Data	cos θ^a, Initial PE	cos θ^a, Treated PE
1	Water	72.8	21.8; 29.1; 21.0; 22.0; 22.1; 25.0; 13.8; 10.8	22.2 ± 1.4	−0.28	0.60
2	Glycerol	63.4	37.4; 37.0; 32.4; 20.5	26.5 ± 1.7	−0.10	0.68
3	Formamide	58.2	39.5; 35.1; 32.0; 28.2; 27.8; 18.1	30.3 ± 1.9	0.05	0.86
4	Ethylene glycol	47.7	30.1; 29.0; 28.7; 28.6; 24.9; 17.5	25.3 ± 1.6	0.17	0.89
5	2,2′-Thiodiethanol	54.0	39.2	35.2 ± 2.2	0.21	0.86
6	Diiodomethane	50.8	48.5	40.5 ± 2.6	0.39	0.61
7	Dimethyl sulfoxide	45.0	25.4	28.2 ± 1.8	0.32	0.83
8	Nitrobenzene	43.9	—	39.7 ± 2.5	0.59	0.88
9	Acetophenone	40.1	—	43.6 ± 2.8	0.67	0.95
10	1-Methylnaphthalene	44.6	—	44.6[b]	0.71	0.80
11	Hexachloro-1,3-butadiene	36.0	35.8	36.0[b]	0.68	0.92
12	1,1,2,2-Tetrabromoethane	47.5	44.3	47.5[b]	0.71	0.91
13	1-Bromonaphthalene	44.6	44.0	44.6[b]	0.71	0.91

[a] The accuracy of cos θ in all cases in ±0.03.
[b] Substances for which the equality $\gamma_l = \gamma_l^d$ is assumed (see text).

threads, and placed at different distances from electrodes. Besides, longer tubes (130 mm) after treatment were cut at different distances from the ends and the wettability was tested at cuts. The invariable value of cos θ in all the cases has allowed us to conclude that the adhesion properties of the internal surface of a treated tube are the same all over its length and are independent of the tube position in the reactor during the treatment.

With the treatment, there is no glow discharge inside the tube. So, to account for the invariable cos θ value, one should suppose that the surface is modified due to reaction with long-lived reactive plasma particles. Note that similar effects have been mentioned in the literature and are used in the remote-plasma reactor,[29] wherein the samples to be treated are situated at a distance of 24 cm from the discharge zone.

Measurement results for a series of liquids in untreated and in treated PE tubes are presented in Table I. To employ the widest possible set of liquids and compare our results with data obtained by other authors, we used the following expedient: Among the liquids we used there are four substances that can be regarded as practically nonpolar ones: 1-methylnaphthalene, hexachloro-1,3-butadiene, 1,1,2,2-tetrabromoethane, and 1-bromonaphthalene. Assuming for these liquids and for untreated PE $\gamma^p = 0$ (and, hence, $\gamma = \gamma^d$) and using eq. (4), from the contact angles θ and surface tensions γ_l of the above-mentioned liquids, we have obtained that for

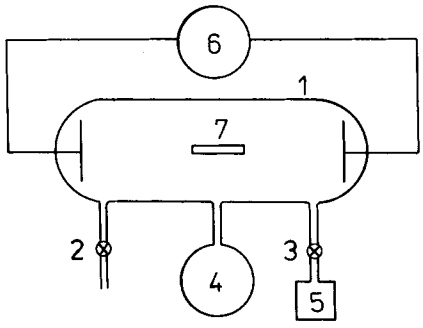

Figure 3 A schematic diagram of the setup for plasma treatment of polymers: (1) glass reactor; (2, 3) cocks for control over gas flow velocity; (4) manometer; (5) vacuum pump; (6) power supply; (7) polymeric sample.

untreated PE $\gamma_s = 30.9 \pm 4.0$ erg/cm^2. This is consistent with the available values 33.1,[17] 34.7,[21] and 31.0[30] erg/cm^2. Then, substituting this value, $\cos\theta$, and γ_l for each of the rest liquids into eq. (4), we have obtained the contributions of the dispersion forces γ_l^d to the surface tensions of these liquids (Table I). Table I also lists γ_l^d values reported in the literature. Our value is seen to be in satisfactory agreement with data obtained by other authors.

Using γ_l^d values obtained in this work, γ_l values reported by other authors, and $\cos\theta$ values measured for treated PE, we have found the γ_s and γ_s^d values showing the best fit to eq. (4) for all the liquids. Thus, for treated PE, we have obtained $\gamma_s = (47.5 \pm 2.0)$ erg/cm^2 and $\gamma_s^d = (35.0 \pm 2.5)$ erg/cm^2.

DISCUSSION

The change in the surface properties of a polymer after glow discharge treatment is associated with chemical modification of the subsurface layer of the polymer.[14,21,31,32] In a $(\gamma^p)^{0.5}$ vs. $(\gamma^d)^{0.5}$ diagram (Fig. 4), the obtained energetic characteristics of initial and plasma-treated PE are marked as points E and T, respectively. The air glow discharge plasma treatment is seen to increase substantially the polar component of the PE surface energy, with the dispersion component being practically unchanged. This result is a characteristic of other discharge-treated polymers as well[15,21,33] and is associated with the formation of oxygen-containing and nitrogenated polar groups at the surface.

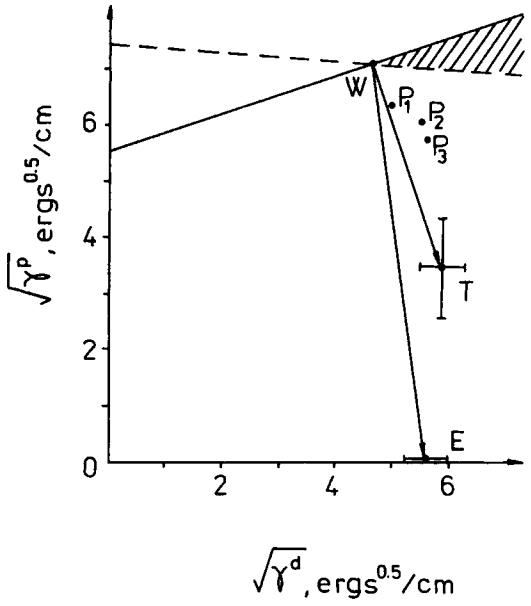

Figure 4 Experimental results and their analysis in terms of a $(\gamma^p)^{0.5}$ vs. $(\gamma^d)^{0.5}$ diagram. Points: E, initial PE; T, plasma-treated PE; P_1, fibrinogen; P_2, γ-globulin; P_3, albumin; W, water. Shaded area, substances for which the adhesion energy at the surface of treated PE in aqueous medium is positive and is higher than that at the surface of initial PE.

We will discuss now the changes in adhesion characteristics of PE under plasma treatment. Let us demonstrate that the effect of plasma reduces the adhesion energy for a wide class of substances in aqueous medium. This can be the reason for the increase in hemocompatibility of the material after plasma treatment.[14] The letters in Figure 4 designate the points corresponding to the following substances: W, water; P_1, fibrinogen; P_2, γ-globulin; and P_3, albumin (data of Paul and Sharma[6]). Note the following peculiarities:

1. WT is shorter than WE. This, according to eq. (25), testifies to an approximately fourfold decrease in polymer–water interfacial tension after treatment.
2. The adhesion energy of each of the three proteins at the polymer surface in an aqueous environment decreases after treatment almost by a factor of 2. According to eq. (30), this manifests itself in the difference of the scalar products $\mathbf{WE} \cdot \mathbf{WP}_i$ and $\mathbf{WT} \cdot \mathbf{WP}_i$.
3. The glow discharge plasma treatment decreases the adhesion energy of every substance X in an aqueous environment if the position of the corresponding point in the diagram meets the condition $\mathbf{WE} \cdot \mathbf{WX} > \mathbf{WT} \cdot \mathbf{WX}$. This inequality is satisfied by the points below the straight line passing through W and perpendicular to $\mathbf{ET}$ (broken line in Fig. 4). Points above the straight line passing through W and perpendicular to $\mathbf{WT}$ correspond to the negative values of adhesion energy at the treated PE surface. Thus, at the treated PE surface, an increase in positive adhesion energy relative to that at the untreated PE surface will be observed only for substances whose points fall within the shaded area in Figure 4. As seen, that is the range of high surface tension (higher than that of water). Hence, one may assume with high probability that the biologic liquid components, whose adhesion determines the biocompatibility of polymers, do not belong to this class, and for them, as for the proteins P_1, P_2, and P_3, the adhesion energy decreases

after plasma treatment. This seems to be the reason for the enhancement of the biocompatibility of polymeric implants after the air plasma treatment.

Materials of both high and low surface energies have been established to show good biocompatibility.[8] In this connection, it is interesting to compare the properties of a plasma-modified surface with those of a hypothetical substance *O* with zero surface energy. The broken line in Figure 5 corresponds to substances with equal values of adhesion energy in an aqueous medium at the surfaces of treated PE and hypothetical substance *O*. Areas on both sides of the line are marked with the inequalities $W_T^a > W_O^a$ and $W_T^a < W_O^a$ in accordance with the values of adhesion energy ratio. For the proteins P_1, P_2, and P_3, these values practically coincide, as seen from the short distance from the points P_i to the straight line. At the same time, the region $W_T^a < W_O^a$ is populated with real substances more densely. For instance, all the liquids we used (except for water) fall within this very region. This may testify to the higher biocompatibility of the hydrophilic substance *T* compared with that of the low-energy substance *O*.

As mentioned above, the theoretically possible decrease in interfacial tension at the polymer–water interface to zero would result in zero adhesion energy

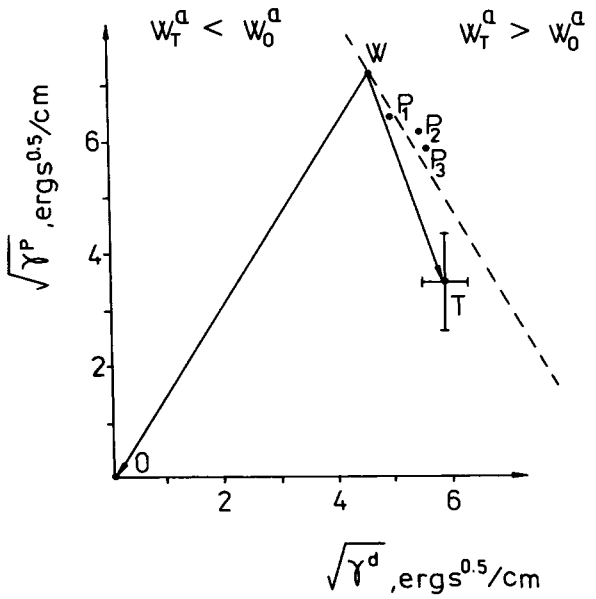

Figure 5 Properties of treated PE compared with those of a hypothetical substance *O* with zero surface energy. The broken line corresponds to substances with equal values of adhesion energy at treated PE and hypothetical substance *O* in aqueous medium.

for any substance in aqueous medium, i.e., it would enhance substantially the biocompatibility of the polymers. Hence, materials with zero interfacial tension have an obvious advantage (from the viewpoint of biocompatibility) over materials with low surface energy.

The geometric method for analyzing the adhesion characteristics of three-component systems might be applicable to consideration of some other problems as well. Thus, for example, it could be applied to treatment of fabrics in order to make them dirt-repellent.[34] The consideration given above shows that a fabric modification decreasing the interfacial tension of the water–fabric interface will result in easier dirt removal from the fabric in washing. Another example is the synthesis of separating membranes. Substance permeation through a membrane involves adsorption at the membrane surface. Affecting this process, one can change the selectivity of membrane separation.

CONCLUSION

We have discussed the geometric approach to analyzing the adhesiveness and other properties of a surface, depending on its energetic characteristics. Desired values are found from a $(\gamma^p)^{0.5}$ vs. $(\gamma^d)^{0.5}$ diagram, wherein corresponding points of interacting substances are laid off. A hypothesis has been used assuming that materials which show low adhesion with respect to the components solved or dispersed in biologic liquids are highly biocompatible. An analysis of interfacial energy characteristics preferable for high biocompatibility of materials has been performed in terms of this hypothesis. It has been shown that at a surface, for which the interfacial tension at the solid–liquid interface is zero, any substance in aqueous medium has zero adhesion energy. This supports the assumption about the high biocompatibility of materials with zero interfacial tension at the solid–water interface. Such materials are preferable to those with low surface energy. Using the above hypothesis, we have considered the physicochemical aspect of the enhancement of PE biocompatibility, resulting from treatment by air glow discharge plasma. The numerical values of the energetic characteristics of the PE surface, obtained from contact angles for a number of liquids, have been reported. The treatment of PE by air glow discharge plasma has been shown to significantly decrease the interfacial tension of the polymer–water interface. For a large number of substances, this leads to decreased adhesion at the polymer surface

in aqueous medium, which we believe is just what increases the biocompatibility of the polymer after the described treatment.

REFERENCES

1. D. H. Kaelble and J. Moacanin, *Polymer,* **18,** 475 (1977).
2. J. D. Andrade, R. N. King, D. E. Gregonis, and D. L. Coleman, *J. Polym. Sci. Polym. Symp.,* **66,** 313 (1979).
3. Y. Ikada, M. Suzuki, and Y. Tamada, in *Polymeric Biomaterials. Proceedings of the Symposium,* Seattle, WA, March 22–25, 1983, Plenum Press, New York, London, p. 135.
4. M. Kumakura and I. Kaetsu, *J. Mater. Sci.,* **21,** 3179 (1986).
5. H. Yasuda, M. O. Bumgarner, H. C. Marsh, et al., *J. Biomed. Mater. Res.,* **9,** 629 (1975).
6. L. Paul and C. P. Sharma, *J. Colloid Interface Sci.,* **84,** 546 (1981).
7. B. Jansen, H. Steinhauser, and W. Prohaska, *Makromol. Chem. Macromol. Symp.,* **5,** 237 (1986).
8. R. E. Baier, *Bull. N.Y. Acad. Med.,* **48,** 257 (1972).
9. D. Kiaei, A. S. Hoffman, B. D. Ratner, T. A. Horbett, and L. O. Reynolds, in *Polymer Material Science and Engineering, Proceedings of the ASC Division of Polymer Material Science and Engineering,* Spring Meeting, Denver, CO, 1987, American Chemical Society, Washington, DC, Vol. 56, 1987, p. 710.
10. D. Klee, W. Breuers, M. Bilo-Jung, et al., *Angew. Makromol. Chem.,* **166/167,** 179 (1989).
11. E. Yano, T. Komai, T. Kawasaki, et al., *J. Biomed. Mater. Res.,* **19,** 863 (1985).
12. B. Jansen, H. Steinhauser, and W. Prohaska, *Angew. Makromol. Chem.,* **164,** 115 (1988).
13. D. W. Fakes, J. M. Newton, J. F. Watts, and M. J. Edgell, *Surf. Interface Anal.,* **10,** 416 (1987).
14. A. M. Gonchar, A. K. Petrov, V. I. Deribas, S. I. Smirnykh, P. I. Parakhina, and A. I. Susoikin, *Bull. SO AMN SSSR,* **6,** 51 (1986).
15. A. K. Petrov, L. F. Vlasova, and V. A. Bagryanskii, *Izvest. SO AN SSSR, Ser. Khim. Nauk,* **4,** 118 (1988).
16. F. M. Fowkes, D. C. McCarthy, and M. A. Mostafa, *J. Colloid Interface Sci.,* **78,** 200 (1980).
17. D. K. Owens and R. C. Wendt, *J. Appl. Polym. Sci.,* **13,** 1741 (1969).
18. J. W. Emsley, J. Feeney, and L. H. Sutcliffe, *High Resolution Nuclear Magnetic Resonance Spectroscopy,* Vol. 2, Pergamon Press, Oxford, 1966, Chap. 10.
19. L. A. Girifalco and R. J. Good, *J. Phys. Chem.,* **61,** 904 (1957).
20. J. O. Hirschfelder, Ch. F. Curtiss, and R. B. Bird, *Molecular Theory of Gases and Liquids,* John Wiley & Sons, New York, London, 1954, Chap. 13.
21. T. Wakida, H. Kawamura, J. C. Song, T. Goto, and T. Takagishi, *Sen-i-gakkaishi, J. Soc. Fiber. Sci. Technol., Jpn.,* **43,** 384 (1987).
22. F. M. Fowkes, *Ind. Eng. Chem.,* **56,** 40 (1964).
23. M. Yu. Pletnev and N. B. Tereschenko, *Ukrainskii Khim. Zh.,* **52,** 427 (1986).
24. R. J. Good, *Adv. Chem. Ser.,* **43,** 74 (1964).
25. A. W. Neuman, R. J. Good, C. J. Hope, and M. Sejpal, *J. Colloid Interface Sci.,* **49,** 291 (1974).
26. S. Wu, *J. Adhesion,* **5,** 39 (1973).
27. M. Saito and A. Yabe, *Text. Res. J.,* **53,** 54 (1983).
28. W. A. Zisman, *Adv. Chem. Ser.,* **43,** 1 (1964).
29. R. Foerch, N. S. McIntyre, R. N. S. Sodhi, and D. H. Hunter, *J. Appl. Polym. Sci.,* **40,** 1903 (1990).
30. H. W. Fox and W. A. Zisman, *J. Coll. Sci.,* **7,** 428 (1952).
31. T. J. Hook, J. A. Gardella, and L. Salvati, *J. Mater. Res.,* **2,** 117 (1987).
32. S. I. Ivanov and V. P. Pechenyakova, *Bulg. J. Phys.,* **11,** 340 (1984).
33. J. B. Donnet, M. Brendle, T. L. Dhami, and O. P. Bahl, *Carbon,* **24,** 757 (1986).
34. C. J. Jahagirdar and S. Venkatakrishan, *J. Appl. Polym. Sci.,* **41,** 117 (1990).

Received July 9, 1991
Accepted April 30, 1992